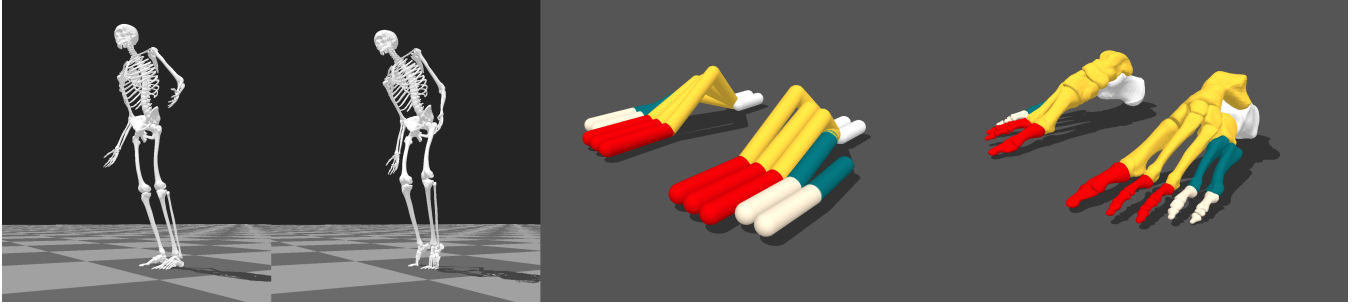# Multi-Segment Foot Modeling for Human Animation

Hwangpil Park
hppark@mrl.snu.ac.kr
Seoul National University

Ri Yu
yuri@mrl.snu.ac.kr
Seoul National University

Jehee Lee*
jehee@mrl.snu.ac.kr
Seoul National University

Figure 1: Left: Tiptoe motion, Center: capsule-shaped multi-segment foot model, Right: skeleton-rendered foot model. We divided our foot model into five segments. Each segment is displayed in a different color. Each capsule is an artificial bone that belongs to exactly one segment and is used as a collision unit.

ABSTRACT

We present a multi-segment foot model and its control method for the simulation of realistic bipedal behaviors. The ground reaction force is the only source of control for a biped that stands and walks on its feet. The foot is the body part that interacts with the ground and produces appropriate actuation to the body. Foot anatomy features 26 bones and many more muscles that play an important role in weight transmission, balancing posture and assisting ambulation. Previously, the foot model was often simplified into one or two rigid bodies connected by a revolute joint. We propose a new foot model consisting of multiple segments to accurately reproduce human foot shape and its functionality. Based on the new model, we developed a foot pose controller that can reproduce foot postures that are generally not obtained in motion capture data. We demonstrate the validity of our foot model and the effectiveness of our foot controller with a variety of foot motions in a physics-based simulation.

CCS CONCEPTS

• **Computing methodologies → Physical simulation**;

KEYWORDS

Human animation, Physical simulation, Biological modeling

*Corresponding Author

1 INTRODUCTION

Reproducing realistic movement of a character in a physics-based simulation is a primary issue in computer graphics and robotics society. Realistic modeling of characters not only makes their appearance look more realistic but also helps simulated behavior to work more feasibly.

The foot is the body part that directly interacts with the ground when standing, walking or running. The human foot contains 26 bones and 33 joints, and more than a hundred of muscles and ligaments. These components form a complicated structure of the foot and move organically to perform various foot functions. For example, the foot can alleviate the shock felt when walking on the ground, provide balance by changing the way it supports the body when standing, and can gain momentum by pushing the ground strongly to increase speed.

Despite these functions of the foot when controlling a biped character, the importance of foot modeling has been overlooked and foot models have not been developed well. As a result, the foot models of biped characters used in physics simulations have mostly consisted of one or two boxes. These types of models cannot reproduce a human foot shape and motions well because they lack sufficient degrees of freedom (DoFs).

In this paper, we propose a new human foot model based on real human foot anatomy, and an algorithm that changes the shape of the foot model depending on a human motion. By using our new foot model and the foot shape controlling method, we can represent the foot shapes and motions better than the existing foot models.

The main contribution of our work is that we created a new foot model that consists of several segments. By designing a foot model

into several pieces, we can reproduce the shape of the various poses that a human foot can achieve. Moreover, because there are many contact points between the foot and the ground, it is possible to enhance the stability of the foot. Another contribution is that we can create the foot motion without extra foot motion data. Previously, because the foot was treated as a simple body, there has been little motion data information available for the foot. In particular, motion capture data deal only with information about the ankle joint. Using our foot model and control method, we can generate the foot motion without detailed motion data of the foot.

In the following sections, we explain our multi-segment model and foot pose control method. Our foot model is based on a human foot and contains several bones and joints. The model imitates a human foot structure and the characteristics of foot-to-ground collisions without becoming overly complex. We introduce our multi-segment foot model in detail and explain how to construct the foot model in section 3. A human foot can change its shape appropriately to perform functions according to the situation or the environment. We used a simple rule to allow the foot to take an appropriate pose depending on the movements of the character. We describe the foot pose control method in section 4 and its simulation in section 5.

We demonstrated the expressiveness and the robustness of our newly designed foot model by conducting several experiments, which are discussed in section 6. We reproduced several complicated foot motions such as foot circling or tiptoeing motion to show the expressiveness of our model. To prove the robustness of the model against the environment and the perturbations, we changed the terrain or pushed the character using two different foot models (two-segment foot and ours) and compared the results. The results prove that our foot model is more robust than the other.

2 RELATED WORK

Developing an accurate control scheme for an articulated humanoid character in a physics-based simulation is a major problem in computer graphics. Many researchers have tried to reproduce realistic human motions with a physically simulated character by using pre-designed finite state machines [Hodgins et al. 1995; Yin et al. 2007] or motion capture data [da Silva et al. 2008; Lee et al. 2010a, 2014; Liu et al. 2016; Sok et al. 2007; Zordan and Hodgins 2002]. In their works, they used human motion data as a reference for the controller. By using the real human data, the results can show more realistic movements for controlling humanoid characters. Moreover, optimization-based controls, which set several pre-defined high-level objectives, were used to find the optimal actuator values to represent various motions [Geijtenbeek et al. 2013; Ha et al. 2012; Macchietto et al. 2009; Mordatch et al. 2013; Witkin and Kass 1988]. The objectives were usually defined by selected features considered to represent the main principles of human motion, such as center of mass position[Abe et al. 2007], a foot landing position [de Lasa et al. 2010], joint torques minimization [de Lasa et al. 2010], or metabolic energy expenditure [Wang et al. 2012].

Successfully balancing humanoid is a well-known problem in computer animation and robotics. Most of works have controlled the representative physical characteristics, such as the center of mass (CoM), the center of pressure (CoP), and the zero-moment point (ZMP). These characteristics should lie on a base of support that is a convex hull composed of the projection of the contacted bodies (often foot). To control CoM, CoP, and ZMP, hip and ankle strategies [Stephens 2007] inspired by human balance control were used. Linear and angular momentum [Abe et al. 2007; Kajita et al. 2003; Macchietto et al. 2009] were also controlled to regulate CoM and CoP. We used the system of Macchietto et al. [Macchietto et al. 2009], which formulated a quadratic problem to attain desirable linear and angular momentum changes.

Because the foot is an important component that directly interacts with the ground for standing and locomotion, progressive models of the foot were proposed progressively, especially in the area of biomechanics [Carson et al. 2001]. Meglan and Berme [Meglan and Berme 1993] suggested the first foot model that was isolated from the ground. They designed the foot as an one-segment model, and the model features a viscoelastic heel made of a single sphere. A two-segment foot model was also proposed by Gilchrist and Winter [Gilchrist and Winter 1996]. They placed one hinge joint between the metatarsal bones and the phalanges to achieve a smooth transition between the swing phase and the stance phase. Studies were conducted to design the foot model to three segments or more [Lopes et al. 2015; MacWilliams et al. 2003]. However, their major goal was to reproduce and analyze kinetic or kinematic information rather than to achieve realistic foot movement reproduction.

Further, as the number of foot segments has increased, there have been attempts to use various segment shapes instead of a box for computational efficiency. These shapes include a sphere [Millard et al. 2009], an ellipsoid [Koop and Q. Wu 2013; Lopes et al. 2015], and a cylinder [Kecskeméthy 2011]. We designed each foot segment as a capsule to accelerate the computation time for calculating the foot-to-ground collisions and to reflect the structure of foot bones and joints.

In the computer graphics community, contact handling has been executed in the usual way, such as non-sliding or non-penetrating. However, most studies on controlling physically simulated characters have treated the foot as a simple structure such as a box or capsule consisting of one or two bodies. Wang et al. [Wang et al. 2009] used a two-segment foot model, which provides more flexibility when the heel strike or toe-off occurs. Jain and Liu [Jain and Liu 2011] proposed a soft foot model based on the finite element method (FEM). Using their soft foot model, they achieved more robust walking control in simulation. Those foot models improved the robustness of controllers and the quality of the resultant motion, but the shape of the foot was not their main concern. Thus, the purpose of modeling the foot was limited to functional areas. We designed the foot as a multi-segment model enough to represent the several important characteristic foot shapes.

3 MULTI-SEGMENT FOOT MODEL

The human foot has a complex structure consisting of 26 bones, 33 joints, and more than 100 muscles and ligaments. However, in computer graphics, most of the foot models used in previous studies focused on physically simulating biped characters often consisted of one or two bodies [Ha and Liu 2014; Lee et al. 2010b; Wang et al. 2012]. These foot models can hardly reproduce the actual foot shapes that a human can make. For example, foot models

with one or two rigid bodies cannot perform foot rotations, such as pronation and supination. Further, it was difficult for them to control the interaction between the foot and the ground during standing because of the lack of DoFs. Consequently, they cannot reproduce the fine foot movements. We intend to design a multi-segment foot model that can describe various foot movements realistically.

To achieve this goal, we wondered if we should apply the real anatomy of human equally to our model. However, as the foot anatomy is quite complex, controlling such a complex structure would be inefficient, so we agreed that there should be a trade-off between accuracy and efficiency. In addition to efficiency, we have considered the tendency of actual foot movement caused by the foot anatomy. Although the foot is composed of 26 bones, the bones do not move separately because they are strongly connected with ligaments. Looking at the anatomy of the foot, the tarsal bones near the ankle are joined by dozens of ligaments. However, it is not the case with the toes located distal to the foot, so the toe bones have high DoFs, relatively. Based on this feature, we tried to design our foot model more realistically by increasing the number of segments and DoFs.

In order to develop the model for the foot while considering the abovementioned concerns, we referred to biomechanics research. Several studies on foot modeling and segmenting in that field have been reported [Deschamps et al. 2011]. Biomechanics researchers were able to analyze foot anatomy and create a model to meet their needs. Among these studies, we found that some divide the foot along the coronal plane (hind foot, forefoot, and hallux) to measure foot kinematics during gait [Carson et al. 2001; Kidder et al. 1996]. However, these models are not sufficient to represent fine movements, such as inversion/eversion, which appear along the sagittal plane. To obtain more delicate foot information, such as kinematics and kinetics data, Macwilliams et al. [MacWilliams et al. 2003] designed a nine-segment foot model. We decided to use a slightly modified version of this model. We first selected six segments that are in direct contact with the ground (heel, medial and lateral forefoot, first toe, second and third toes, and fourth and fifth toes) and then incorporated the first toe and the second and third toes into one segment for simplicity. Furthermore, we made other segments (talus, navicular and cuneiform) that do not have contact with the ground belong to the medial phalanges, which form an arch of the foot.

To summarize, our foot model consists of five segments and each segment is a control unit. To move each segment properly, we planted four joints (3 DoFs per each joint) in our foot model. A segment is composed of several artificial bones that represent phalanges, metatarsal bones, or the tarsal bones. In the following subsection, we describe the artificial foot bone first, followed by foot segmentation and joint placement in detail.

3.1 Artificial Foot Bones

Human foot bones are largely divided into three parts: tarsal bones, metatarsal bones, and phalanges. Tarsal bones are seven bones that make up the midfoot and the hindfoot. Metatarsal bones are located in the midfoot and phalanges are in the forefoot. Our foot model consists of 16 capsule-shaped artificial bones that correspond to the
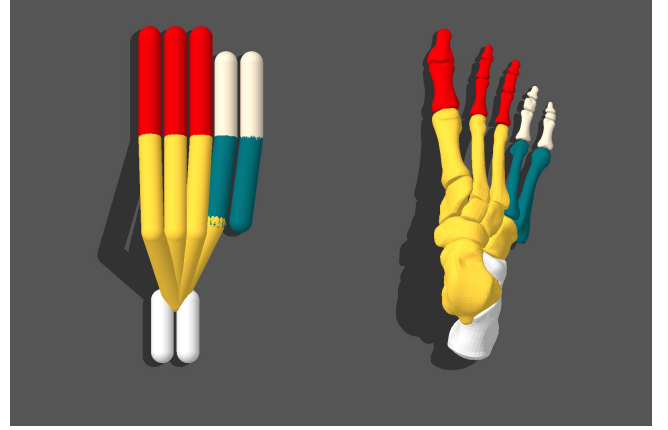
Figure 2: Our multi-segment foot model consists of 16 artificial bones and five segments. Each bone has a capsule shape that is set to have two contact points at most. To help understand, each segment was painted in a different color. red: medial phalanges, ivory: lateral phalanges, yellow: medial metatarsal, green: lateral metatarsal, white: heel.

human foot bones (center of Figure 1). Among the 16 bones, the five bones on the forefoot correspond to phalanges, the other five at the middle are metatarsal bones, and the other two form the calcaneus. We modeled the tarsal bones (colored with yellow in figure 2) but decided not to directly control them for two reasons. One reason is that they rarely come into contact with the ground, so there is no interaction. he second reason is that they experience little movement because they are strongly bonded to the surrounding bones with ligaments.

Metatarsal bones and phalanges have cylindrical shapes. Wedge-shaped metatarsal bones and phalanges can be treated as a cylinder [Patton 2015], so we designed artificial bones with capsule primitives with the same radius. A capsule is a cylinder with hemispheres on both ends. This is often for collision detection. We assume that each artificial bone can collide with the ground. We have made the collision occur only at both ends of the capsule-shaped bone, which are hemispheres.

3.2 Foot Segmentation

We divided the 16 artificial bones into five segments (Figure 2). After observing various foot motions, we found that the individual movements of foot bones are constrained because they are connected to each other with ligaments. Therefore, we grouped bones that are moving and contact the ground together into same segment, and we control our foot model on a segment basis.

We defined five segments with the following names: medial phalanges, lateral phalanges, medial metatarsal, lateral metatarsal, and heel. We defined five segments with the following names: medial phalanges, lateral phalanges, medial metatarsal, lateral metatarsal, and heel. There are four basic foot poses: rest pose, a tiptoe, an inside tilt, and an outside tilt (Figure 3). By making the artificial bones that belong to some segments contact the ground, we can make the foot model achieve one of the basic poses. For stable contact,
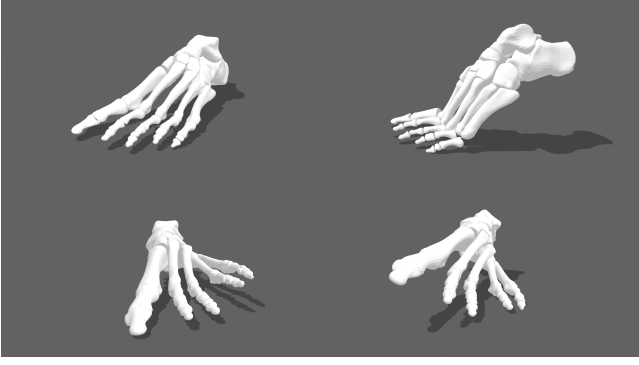
Figure 3: Four basic foot poses. Top left: rest pose, top right: tiptoe, bottom left: inside tilt and bottom right: outside tilt.
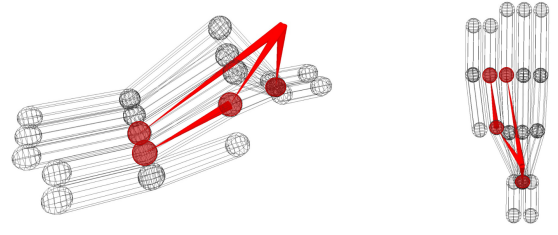

Figure 4: We put four joints (marked with the red circle) on our foot model to move each segment properly. The locations of joints are between the third metatarsal and the third phalanges, between the fourth metatarsal and the fourth the phalanges, between the fourth metatarsal and the cuboid, and on the heel.

we selected the number and the shape of the bones that belong to the segment so that each segment has three or more contact points when contacting with the ground.

3.3 Joint Placement

We put four joints on our foot model to move each segment properly. Each joint is located based on the joint location on a real human foot. We used 3-DoF ball joints for foot joints so the foot model can have 12 DoFs (Figure 4). The location of each joint is between the third metatarsal and the third phalanges, the fourth metatarsal and the fourth the phalanges, the fourth metatarsal and the cuboid, and on the heel.

The place where the foot is bent most is between the toe and the metatarsals. Therefore, we put two joints between the metatarsal bones and the phalanges. Looking at the midfoot during the rest pose from the front, the lateral side of the foot is in contact with the ground while the medial side is in arched form without touching the ground. When the foot tilts to the outside, the lateral metatarsals and heel are in contact with the ground. To control the outside metatarsals, we put a joint between the fourth metatarsal and the cuboid. However, when inside tilt occurs, medial metatarsals are still arched and have no contact or any notable movement, so we decided not to place a joint there. Instead, we made this part subordinate to the ankle joint. The heel joint does not exist on a human foot but we made one for the following reason. The heel is the part that can contact the ground at any pose except the tiptoe pose because of the characteristic shape of the calcaneus bone. The bone can make contact in various directions. To allow our foot model to perform the function of the calcaneus bone, we put a joint on the heel.

All the capsule-shaped artificial bones we designed have the same radius and the end of the bones overlap to form a sphere. We set the joint location to the center of the sphere, and the intersection of two bones are connected by that joint. Because two bones sharing a joint have the same contact point, one calculation for contact per joint is reduced.

4 FOOT POSE CONTROL

When a person is standing on the ground, their foot can be in contact with the ground in various ways (Figure 3). To reproduce

these various shapes and motions of the foot naturally, the foot model must have many DoFs. We made a multi-segment foot model that has 12 DoFs based on human foot shape and have discussed the model in detail in the previous chapter.

Although our foot model has the power to represent various shapes and motions of the foot, the joint angles in the foot should be determined to make specific pose. However, because there was not much concern about the foot modeling until now, when capturing human motion, the foot was not the subject of consideration. In other words, motion capture data describing delicate foot motion are difficult to obtain. Therefore, we need a methodology that can control the foot depending on the environment or desired behavior without reference data of the foot.

Our control strategy for the foot model utilizes foot pose control. By using the foot pose controller, we reproduce an appropriate foot pose for a given ankle position and segments that are specified by the user to be in contact with the ground.

We considered an ankle position and the contacting segments to decide the foot shape at each moment because we considered it was sufficient to express the foot pose. For example, the tiptoe pose can be made by setting a high ankle position and making the toe segments attached to the ground and vice versa. Our foot model is embedded in the existing biped character model. The ankle joint position is obtained from the motion data, and the segments that must have contact with the ground for the task are provided by a user. Because the inputs of our controller can be obtained without detailed information about foot motion, we can reconstruct the foot pose together with the full body pose by common motion capture data.

Foot pose control proceeds in the following order (Figure 5). First, place the ankle joint at the ankle position of the motion capture data. Next, adjust the orientation of the ankle joint to place the joint belonging to the segment entered as the control input on the ground. Lastly, rotate the joint belonging to the segment in order to make the bones in input-segment be parallel with the ground.

The joint orientations can be obtained by the following calculation. Let $\vec{p}_a$ be ankle joint position, and $\vec{p}_s$ be joint position of marked segment. Now we let $\vec{v}_{sa} = \vec{p}_s - \vec{p}_a$. To change the original ankle orientation as little as possible in the motion capture data, we try to rotate the ankle joint to the smallest angle so that
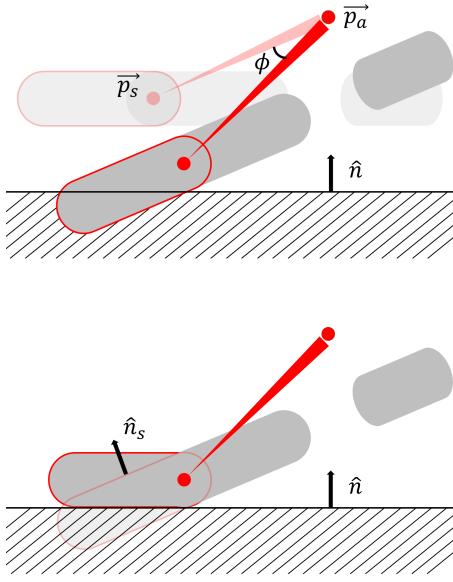
Figure 5: Foot pose control process. For clarity, we draw our foot model in 2D. An artificial bone marked with the red border is the one belonging to the selected segment to contact with the ground. Up: We rotate the ankle joint to make the selected segment joint touch the ground. Bottom: We rotate the selected segment joint to make the selected bone parallel to the ground.

the segment joint could touch the ground. A rotation axis of the smallest rotation to make the segment joint touched the ground is perpendicular to the plane which contain $\vec{v}_{sa}$ and $\hat{n}$, where the rotation axis is perpendicular to $\vec{v}_{sa}$ and $\hat{n}$. The rotation axis $\hat{\omega}$ can be obtained as follows.

$$\hat{\omega} = \frac{\hat{n} \times \vec{v}_{sa}}{\|\hat{n} \times \vec{v}_{sa}\|} \tag{1}$$

The rotation angle that causes $\vec{v}_{sa}$ to touch the ground is equal to the value obtained by subtracting the angle between $\vec{v}_{sa}$ and $-\hat{n}$ from the angle between $\vec{v}'_{sa}$ and $-\hat{n}$ where $\vec{p}_a + \vec{v}'_{sa} - r_c\hat{n}$ is on the ground. When ankle joint is rotated at angle ϕ, segment joint can touch the ground.

$$\phi = atan2(\left\|\vec{v}_{sa} - (\vec{v}_{sa} \cdot \hat{n})\hat{n}\right\|, \ -\vec{v}_{sa} \cdot \hat{n}) - \cos^{-1}(\frac{\vec{p}_a \cdot \hat{n} - r_c}{\|\vec{v}_{sa}\|}) \tag{2}$$

where r_c is a radius of a capsule of each bone.

After the segment joint touches the ground, we should make the bones in the segment be parallel to the ground, not to penetrate the ground. We rotated the segment joint so that the segment normal $\hat{n}_s$ matches the ground normal $\hat{n}$ for that. In this case, we need to determine the remaining direction of the segment. We tried to reduce the unnaturalness by making the direction of the segment coincide with the target direction $\hat{t}$, which is the projection of the

foot direction $\hat{a}$ on the ground plane. We set $\hat{a}$ to be a unit direction from an ankle to a toe in the original motion data.

$$\hat{t} = \frac{\hat{a} - (\hat{a} \cdot \hat{n})\hat{n}}{\|\hat{a} - (\hat{a} \cdot \hat{n})\hat{n}\|} \tag{3}$$

$$R_s = R(\hat{s}, \hat{t})R(\hat{n}_s, \hat{n}) \tag{4}$$

where R_s is rotation that segment joint should be rotated with. $\hat{t}$ is the segment target direction that is calculated from the ankle direction, $\hat{s}$ is the segment direction, and $\hat{n}_s$ is the segment normal unit vector. $R(\hat{c}, \hat{d}) \in R^{3 \times 3}$ is the rotation matrix rotating $\hat{c}$ to $\hat{d}$ with the smallest rotation angle, where

$$R(\hat{c}, \hat{d}) = \exp(\cos^{-1}(\hat{c} \cdot \hat{d})\frac{\hat{c} \times \hat{d}}{\left\|\hat{c} \times \hat{d}\right\|}) \tag{5}$$

The calculation of the pose control of the foot model is performed every time step and it is performed very quickly. Therefore, our controller works in real time.

5 SIMULATION WITH MULTI-SEGMENT FOOT MODEL

We verified that the foot motion is well generated by using the physics-based simulation of applying our foot model and foot pose control. The humanoid character with our foot model simulates the various foot movements obtained by the foot pose control while tracking the standing motion.

We used the balancing system of Macchietto et al. [Macchietto et al. 2009] to keep the humanoid character in balance while standing. Macchietto et al. [Macchietto et al. 2009] used the method to balance by adjusting the linear momentum and the angular momentum of humanoid character. The character maintains its balance if its CoM and CoP are inside the BoS (base of support) which is the convex hull of the bones in contact with the ground. After deciding the desired CoM and CoP according to the positions of bodies contacting the ground, the quadratic optimization problem is defined for moving the current CoM and CoP to the desired position. The output of this optimization is joint angle accelerations. They obtain the joint torques by putting the accelerations into the dynamics solver and solving the floating-base hybrid dynamics. The simulation is performed by applying the obtained joint torques to each joint of the character. The optimization problem is defined below.

$$\ddot{\theta}^* = \underset{\ddot{\theta}}{\text{argmin}} \ w_t C_t + w_l C_l + w_h C_h$$
$$\text{subject to: } a_{sup} = J_{sup}\ddot{\theta} + \dot{J}_{sup}\dot{\theta} \tag{6}$$

where $\dot{\theta}$ and $\ddot{\theta}$ are the joint angle velocities and accelerations, $C_t(\ddot{\theta})$ is a quadratic objective to track the reference motion, $C_l(\ddot{\theta})$ and $C_h(\ddot{\theta})$ are also quadratic objectives to achieve the desired linear and angular momentum changes. J_{sup} is the Jacobian of the supporting bodies, and $\dot{J}_{sup}$ is the time derivative of J_{sup}. w_t, w_l, and w_h are the weights for tracking, linear momentum, and angular momentum objectives, respectively.

Non-slip condition constraints in equation (6) require determined supporting bodies. Because we obtained which segments should be in contact with the ground from the user-input when deciding the foot pose described in the previous section, non-slip constraints

can be calculated using the user-input directly. Those user-input selected segments are corresponding to the supporting bodies in the optimization and using these information, the optimization is processed together with the foot pose control. J_{sup} and $\dot{J}_{sup}$ are calculated for those segments. We set a_{sup} to keep the segments in contact and parallel with the ground in a proportional-derivative (PD) control manner for both linear and angular quantities of the segments.

$$a_{sup} = \begin{pmatrix} k_s(p_{s,ref} - p_s) - d_s v_s \\ k_s \text{diff}(q_{s,ref}, \ q_s) - d_s \omega_s \end{pmatrix} \tag{7}$$

where k_s is a proportional gain, $d_s = 2\sqrt{k_s}$ is a derivative gain, $p_{s,ref}$ and p_s are joint positions in Cartesian coordinates of selected segments for the reference motion and the simulated character, $q_{s,ref}$ and q_s are joint orientations in SO(3) of selected segments for the reference motion and the simulated character, and v_s and ω_s are joint linear and angular velocities in Cartesian coordinates of selected segments for the simulated character. We used $k_s = 28$.

We set the values of θ and $\dot{\theta}$ as a current configuration of the character at the moment of optimization. Because J_{sup} and $\dot{J}_{sup}$ can be calculated from θ and $\dot{\theta}$, the constraints of Equation (6) are linear with respect to $\ddot{\theta}$. Because the objective of Equation (6) is quadratic with respect to $\ddot{\theta}$, the results of the optimization can be obtained by solving a set of linear equations.

6 EXPERIMENTAL RESULTS

Our human model has 66 DoFs (including 12 DoFs of each foot), is 150cm tall, and weighs 48.5kg. We used the dynamic system based on the Lie Group theory [Park et al. 1995] to solve the forward and the inverse dynamics. Our simulation rate is 1800Hz to simulate small segments on the foot model robustly. Foot pose control and optimization for maintaining balance of the character is performed every 30 Hz. The ground reaction forces are calculated by the penalty method using a damped spring model, and the damped coefficients are $k_s = 15000 \ N/m$ and $k_d = 2\sqrt{k_s} \approx 245N \cdot s/m$, respectively.

6.1 Reproducing Various Foot Motions

Using our multi-segment foot model, we can simulate natural, sophisticated foot motions such as tiptoeing, tilting, circling on one foot, and centering on one foot (Figure 6). Given the ankle position and the foot segments that should be in contact with the ground as inputs, the foot pose is decided by our foot pose controller. In the figures and video, the foot bones are shown in red to indicate that the bones are in contact with the ground. Please watch the accompanying video for detailed motion.

Tiptoe. Tiptoeing is an unstable pose because it uses only the front, narrow area of the foot to balance while lifting the heel. The foot models that consist of a single body or two cannot produce the tiptoeing motion properly because they have a small number of contact points. In our experiment, 10 contact points exist in the toe area, and these points are activated by turns according to the COM of the body to balance like a real human does. Therefore, the tiptoe motion looks natural.

Tilt. When a human leans to the side like a skiing motion, the side of the foot comes into contact with the ground. We demonstrate this as foot tilt using our foot model. When we make the foot model tilt to the left side, the upper body is bent to the opposite side for balance. There are some internal collisions between body parts, and we will discuss this issue later.

One Foot Circling. With our multi-segment foot model, delicate foot movement such as foot circling can be produced. When stretching, a person turns their one ankle to release their ankle joint. At this moment, with the heel lifted, the toes touch the ground in turn.

Centering on One Foot. Our model can balance with one foot. We let the character lift the right foot and balance with the left foot only. The character tilts its upper body toward the stance foot and shifts the CoM position to balance.

6.2 Robustness

A human can maintain balance while standing on flat ground, a gravelly field, or rocky terrain. In addition, a human is able to withstand the force of a push. These actions can be achieved by changing the foot pose to suit the situation. We conducted experiments to verify the robustness of our foot model on curved terrain or in a situation where an external force is acting. The results were compared with those obtained using the two-segment foot model.

Rough Terrain. Our foot model can stand on rough terrain as well as flat ground. In order to stand on bumpy ground, the foot must be able to change its shape to fit the terrain. We let the two foot models (two-segment foot and multi-segment foot) stand on sphere-shaped ground and compared the results. When using the two-segment foot model, the simulated character cannot balance on the spherical terrain, and gradually slips. The character that utilizes our multi-segment foot model can balance on this terrain by changing the topology of the foot model. The result of this example shows that our foot model adapts well to the environment in a manner similar to a human (Figure 7).

Moving Slope. We simulated a character standing on a moving slope (Figure 9). As the angle of the slope increases, our foot model flexes the joints between the phalanges and the metatarsal bones to stand on the inclined floor using its toes to balance. This is the similar to how a human would balance on a slope.

External Perturbation. To show the robustness of our controller, we applied a perturbation while the model was standing. We applied the external force to the torso of the character from three different directions (front, side, and back) for 0.4 s. The character with the multi-segment foot model can endure the external force from the front up to 65 N. When the model was pushed from the side, it can withstand 75 N. When it was pushed from the back, it can withstand 50 N.

Further, we compared the resilience of the multi-segment foot model and that of the two-segment foot model (Figure 8). Because the two-segment foot has few DoFs, when an external force is applied, the foot slips off the ground, becomes unstable, and eventually falls. However, our foot model is an articulating body consisting of segments and joints, so it can move like human foot. Therefore, when an external force is applied, only some parts of it fall off
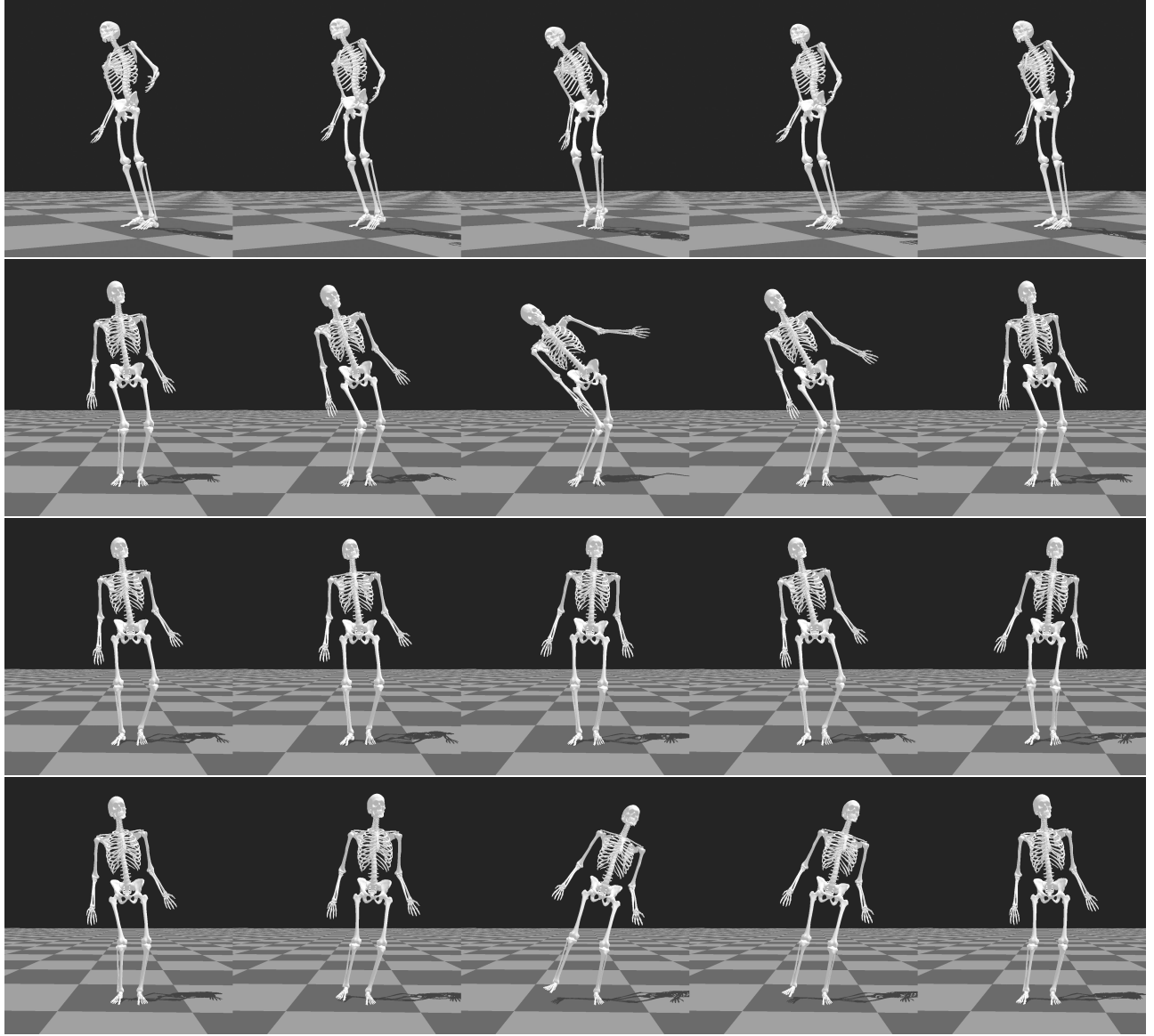
Figure 6: We can simulate various foot motions with our multi-segment foot model: tiptoe, tilt, one foot circling and centering on one foot.

Table 1: We measured the maximum forces that each foot model could withstand. Our multi-segment foot model is more robust than the two-segment foot model. The multi-segment model can endure the external force up to 75 N.

Force(N)	Two-segment	Multi-segment
Front	45	65
Side	50	75
Back	40	50

the ground. Other parts remain on the ground, which makes the overall model more stable. The experimental results confirm that

our multi-segment foot model is more robust than the two-segment foot when forces are applied in any direction (Table 1). We also added more contact points to edges of box in a two-segment foot model and conducted a pushing experiment as well, but we cannot see the differences in reaction.

Virtual Contact Plate. We display the virtual contact plate to show the change in foot contact during the simulation. Through the robustness experiments, we proved that our multi-segment foot model is more robust than the two-segment foot model because our foot model can change its shape and contact points. By visualizing the contact points with the virtual contact plate, we can show the change in foot state more clearly (Figure 10).
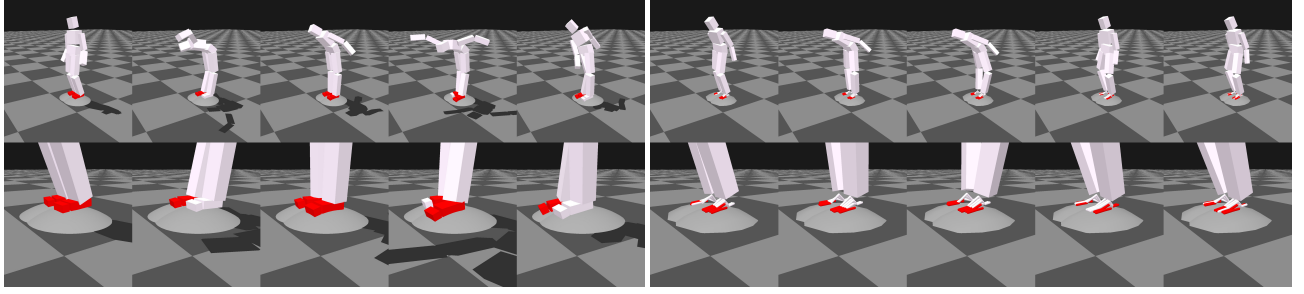
Figure 7: We created bumpy terrain and placed our character on top. The two-segment model (left column) cannot stand on the bumpy terrain stably while our model (right column) can stand stably by properly changing the foot shape according to the terrain.
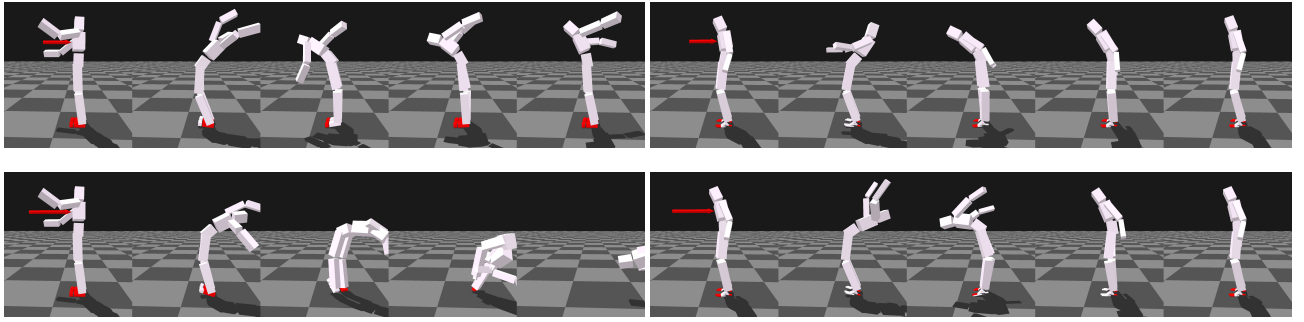

Figure 8: We applied an external force to the character to show the robustness of the controller. We used two foot models, one is the two-segment foot model (left column) and the other is our proposed multi-segment model (right column). An external force of 40 N is applied to the experiment in the first row and 60 N in the second row. The two-segment model cannot endure 60 N force, while our multi-segment model can. Our model can withstand external force through proper adjustment of the foot pose.
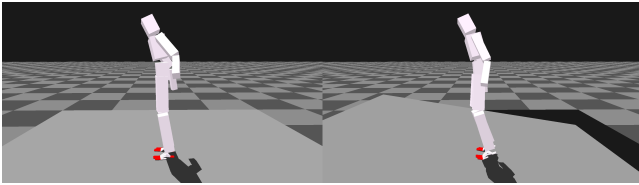

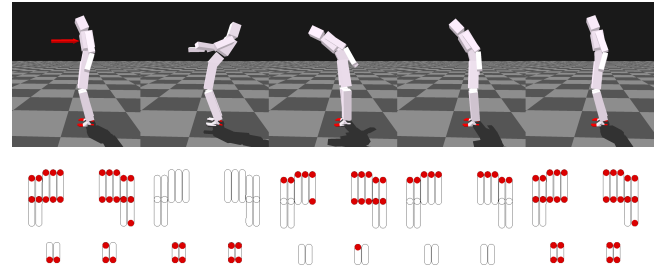
Figure 9: Standing motion on a moving slope.

Figure 10: We displayed the contact points on the virtual contact plate to visualize the change in contact while the human character is pushed by the external force. Note that the medial metatarsal segment was not displayed on the contact plate. This is because the segment is assumed to have no contact with the ground.

7 DISCUSSION

In this paper, we proposed a new foot model that consists of 16 artificial bones and five segments, and we proposed a controller that can successfully manage the interactions between the foot model and the ground. Previous studies on computer graphics tried several control methods to reproduce realistic human movements, but they did not pay much attention to foot modeling. We constructed the multi-segment foot model to resemble a human foot and simulate delicate motions.

For design convenience and computational efficiency, we used the capsule-shaped primitive for every foot bone, and each joint on the foot is a 3-DoF ball joint. Our foot model has more segments and DoFs than the foot models used in the previous works; therefore, we

can generate delicate foot motion such as foot circling. In addition, our foot model is robust enough to adapt to rough terrain or endure external perturbation. We believe that by using our multi-segment foot model, a biped character simulation can be more expressive and robust.
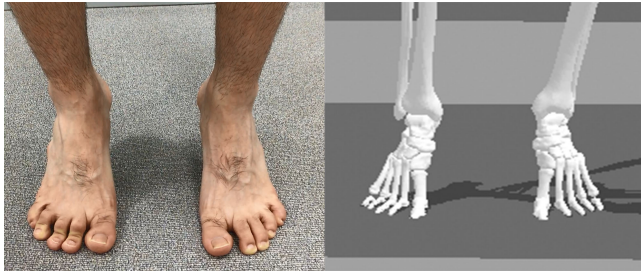
Figure 11: Our foot model can reproduce human foot shapes and movements naturally. The left picture is the human foot tiptoeing and the right picture is tiptoe simulation result. Our controller can generate natural foot motion like human motion.

Although the soft foot model [Jain and Liu 2011] using a soft body simulation based on FEM can achieve robust simulation results, we did not apply FEM to our foot model. We applied our foot model to the existing rigid body character model to exploit the advantages of an articulated rigid body simulation, which include simple calculations and precise articulation.

Our foot modeling approach is meaningful in that we paid attention to the structure of the foot when creating our model; the structure had been previously been regarded as a simple form. Nevertheless, our foot model and the control method also have several limitations. First, we only can generate motions in place. In the near future, we believe we can control walking motion by using our multi-segment foot. Our controller determines the foot pose for the given inputs. The foot is the major body part that takes the contact force from the ground, so we expect that controlling not only the foot pose but also the ground reaction forces makes system more stable. We will build a controller that can directly control the ground reaction force. We currently use a penalty-based method for the computation of ground reaction force. For precise interaction between the foot and the ground, it is better to use the constraint-based method, such as LCP, to calculate contact force.

In addition to the drawbacks in simulation, there are some issues regarding foot modeling. We divided a foot into small pieces for expressiveness, but this can cause a problem. Because each bone in the foot model has a relatively small mass, the simulation will be unstable when a strong ground reaction force is generated. Therefore, we used a small time step for dynamics integration. To control the foot model conveniently, we grouped the bones according to the movement of the foot. However, the foot movement of the grouped bones may seem unnatural in some cases. For example, in "rough terrain" experiments, it is natural for the toes to touch the ground all the way to grab the rounded ground. However, we grouped three toes (marked in red in Figure 2) together and treated them as one rigid body. All the bones in this segment, called medial phalanges, rotate together such that some of the bones in that segment cannot reach the ground. We decided to control the foot model on a segmented basis because the foot bones are strongly connected by ligaments. However, because the phalanges have a high DoF, it is better to control them individually rather than to group them

together. Inevitably, the foot model needs to be further subdivided and controlled for more natural foot motion.

In some examples, especially the "tilt" example, self collisions occurred. For computational convenience, we did not consider the joint limit and self collisions. Because setting the joint limit and avoiding self collisions can make the simulated character motions more realistic, it would be desirable to consider these issues in the next study.

An actual human foot has a very complex structure composed of dozens of bones and hundreds of muscles and ligaments. In particular, the bones that comprise the foot are not separated from each other; they are joined together by ligaments. Hence, they can interact flexibly without major changes in shape. Recently, studies controlling human character using muscles have been successful [Lee et al. 2018, 2014]. For more precise foot control, foot modeling with muscles is an interesting research topic. Using muscles for foot modeling can explain many things about foot movement. In addition, we expect that studies about the human hand will be a good reference for further research about foot structure and movement [Sachdeva et al. 2015].

ACKNOWLEDGMENTS

REFERENCES

Yeuhi Abe, Marco da Silva, and Jovan Popović. 2007. Multiobjective Control with Frictional Contacts. In *Proceedings of the 2007 ACM SIGGRAPH/Eurographics Symposium on Computer Animation (SCA '07)*. 249–258.

MC Carson, ME Harrington, N Thompson, JJ O'connor, and TN Theologis. 2001. Kinematic analysis of a multi-segment foot model for research and clinical applications: a repeatability analysis. *Journal of biomechanics* 34, 10 (2001), 1299–1307.

Marco da Silva, Yeuhi Abe, and Jovan Popović. 2008. Interactive Simulation of Stylized Human Locomotion. *ACM Trans. Graph.* 27, 3 (2008), 82:1–82:10.

Martin de Lasa, Igor Mordatch, and Aaron Hertzmann. 2010. Feature-based Locomotion Controllers. *ACM Trans. Graph.* 29, 4, Article 131 (2010), 131:1–131:10 pages.

Kevin Deschamps, Filip Staes, Philip Roosen, Frank Nobels, Kaat Desloovere, Herman Bruyninckx, and Giovanni A Matricali. 2011. Body of evidence supporting the clinical use of 3D multisegment foot models: a systematic review. *Gait & posture* 33, 3 (2011), 338–349.

Thomas Geijtenbeek, Michiel van de Panne, and A. Frank van der Stappen. 2013. Flexible Muscle-based Locomotion for Bipedal Creatures. *ACM Trans. Graph.* 32, 6 (2013), 206:1–206:11.

L.A. Gilchrist and D.A. Winter. 1996. A Two-Part, Viscoelastic Foot Model for use in Gait Simulations. 29, 6 (1996), 795–798.

Sehoon Ha and C Karen Liu. 2014. Iterative training of dynamic skills inspired by human coaching techniques. *ACM Transactions on Graphics (TOG)* 34, 1 (2014), 1.

Sehoon Ha, Yuting Ye, and C. Karen Liu. 2012. Falling and Landing Motion Control for Character Animation. *ACM Trans. Graph.* 31, 6 (2012), 155:1–155:9.

Jessica K. Hodgins, Wayne L. Wooten, David C. Brogan, and James F. O'Brien. 1995. Animating Human Athletics. In *Proceedings of the 22Nd Annual Conference on Computer Graphics and Interactive Techniques (SIGGRAPH '95)*. 71–78.

Sumit Jain and C. Karen Liu. 2011. Controlling Physics-based Characters Using Soft Contacts. *ACM Trans. Graph.* 30, 6, Article 163 (2011), 163:1–163:10 pages.

S. Kajita, F. Kanehiro, K. Kaneko, K. Fujiwara, K. Harada, K. Yokoi, and H. Hirukawa. 2003. Resolved momentum control: humanoid motion planning based on the linear and angular momentum. In *Proceedings 2003 IEEE/RSJ International Conference on Intelligent Robots and Systems (IROS 2003) (Cat. No.03CH37453)*, Vol. 2. 1644–1650 vol.2.

A Kecskeméthy. 2011. A novel cylinder-plane foot contact model for human gait motion reproduction. In *Proc. ECCOMAS Thematic Conf. on Multibody Dynamics, Brussels, Belgium*.

Steven M Kidder, Faruk S Abuzzahab, Gerald F Harris, and Jeffrey E Johnson. 1996. A system for the analysis of foot and ankle kinematics during gait. *IEEE Transactions on Rehabilitation Engineering* 4, 1 (1996), 25–32.

Derek Koop and Christine Q. Wu. 2013. Passive Dynamic Biped Walking-Part I: Development and Validation of an Advanced Model. 8 (10 2013), 041007.

Seunghwan Lee, Ri Yu, Jungnam Park, Mridul Aanjaneya, Eftychios Sifakis, and Jehee Lee. 2018. Dexterous Manipulation and Control with Volumetric Muscles. *ACM Trans. Graph.* 37, 4 (2018).

Yoonsang Lee, Sungeun Kim, and Jehee Lee. 2010a. Data-driven Biped Control. *ACM Trans. Graph.* 29, 4, Article 129 (July 2010), 129:1–129:8 pages.

Yoonsang Lee, Sungeun Kim, and Jehee Lee. 2010b. Data-driven biped control. *ACM Transactions on Graphics (TOG)* 29, 4 (2010), 129.

Yoonsang Lee, Moon Seok Park, Taesoo Kwon, and Jehee Lee. 2014. Locomotion Control for Many-muscle Humanoids. *ACM Trans. Graph.* 33, 6, Article 218 (2014), 218:1–218:11 pages.

Libin Liu, Michiel Van De Panne, and Kangkang Yin. 2016. Guided Learning of Control Graphs for Physics-Based Characters. *ACM Trans. Graph.* 35, 3, Article 29 (2016), 29:1–29:14 pages.

Daniel Lopes, Rick Neptune, Jorge Ambrósio, and Miguel Silva. 2015. A superellipsoid-plane model for simulating foot-ground contact during human gait. 19 (2015), 1–10.

Adriano Macchietto, Victor Zordan, and Christian R. Shelton. 2009. Momentum Control for Balance. *ACM Trans. Graph.* 28, 3, Article 80 (2009), 80:1–80:8 pages.

Bruce A. MacWilliams, Matthew Cowley, and Diane E. Nicholson. 2003. Foot kinematics and kinetics during adolescent gait. *Gait & Posture* 17, 3 (2003), 214–224.

D. Meglan and N. Berme. 1993. A 3D passive mechanical model of the human foot for use in locomotion synthesis. *Journal of Biomechanics* 26, 3 (1993), 331.

Matthew Millard, John McPhee, and Eric Kubica. 2009. *Multi-Step Forward Dynamic Gait Simulation.* 25–43.

Igor Mordatch, Jack M. Wang, Emanuel Todorov, and Vladlen Koltun. 2013. Animating Human Lower Limbs Using Contact-invariant Optimization. *ACM Trans. Graph.* 32, 6 (2013), 203:1–203:8.

F. C. Park, J. E. Bobrow, and S. R. Ploen. 1995. A Lie Group Formulation of Robot Dynamics. *Int. J. Rob. Res.* 14, 6 (1995), 609–618.

Kevin T. Patton. 2015. *Anatomy & Physiology.*

Prashant Sachdeva, Shinjiro Sueda, Susanne Bradley, Mikhail Fain, and Dinesh K. Pai. 2015. Biomechanical Simulation and Control of Hands and Tendinous Systems. *ACM Trans. Graph.* 34, 4 (2015), 42:1–42:10.

Kwang Won Sok, Manmyung Kim, and Jehee Lee. 2007. Simulating Biped Behaviors from Human Motion Data. *ACM Trans. Graph.* 26, 3, Article 107 (2007).

B. Stephens. 2007. Integral control of humanoid balance. In *2007 IEEE/RSJ International Conference on Intelligent Robots and Systems.* 4020–4027.

Jack M. Wang, David J. Fleet, and Aaron Hertzmann. 2009. Optimizing Walking Controllers. *ACM Trans. Graph.* 28, 5, Article 168 (2009), 8 pages.

Jack M. Wang, Samuel R. Hamner, Scott L. Delp, and Vladlen Koltun. 2012. Optimizing Locomotion Controllers Using Biologically-based Actuators and Objectives. *ACM Trans. Graph.* 31, 4, Article 25 (2012), 25:1–25:11 pages.

Andrew Witkin and Michael Kass. 1988. Spacetime Constraints. *SIGGRAPH Comput. Graph.* 22, 4 (1988), 159–168.

KangKang Yin, Kevin Loken, and Michiel van de Panne. 2007. SIMBICON: Simple Biped Locomotion Control. *ACM Trans. Graph.* 26, 3, Article 105 (2007).

Victor Brian Zordan and Jessica K. Hodgins. 2002. Motion Capture-driven Simulations That Hit and React. In *Proceedings of the 2002 ACM SIGGRAPH/Eurographics Symposium on Computer Animation.* 89–96.